

Surface chemical and electronic properties of plasma-treated n-type $\text{Al}_{0.5}\text{Ga}_{0.5}\text{N}$

X. A. Cao^{*1}, H. Piao², J. Li³, J. Y. Lin³, and H. X. Jiang³

¹ Department of Computer Science and Electrical Engineering, West Virginia University, Morgantown, WV 26506, USA

² GE Global research Center, Niskayuna, New York 12309, USA

³ Department of Physics, Kansas State University, Manhattan, KS 66506, USA

Received 4 April 2007, revised 3 July 2007, accepted 5 July 2007

Published online 7 September 2007

PACS 61.80.Jh, 73.40.Kp, 79.60.Bm, 81.65.Cf

The effects of plasma treatment on the surface properties of Si-doped $\text{Al}_{0.5}\text{Ga}_{0.5}\text{N}$ were studied by X-ray photoelectron spectroscopy and metal contact measurements. Plasma treatment resulted in a N-deficient nonstoichiometric AlGa_N surface with an increased O concentration and large red shifts of photoelectron peaks. The red shifts remained after removal of the surface oxide, indicating a downward shift of the surface Fermi level as a result of ion-induced compensating defects. Pre-metal plasma treatment led to more rectifying electrical characteristics of Ti/Al/Ti/Au contacts. Current–voltage characterization at elevated temperatures revealed strong compensating effects of the plasma damage in $\text{Al}_{0.5}\text{Ga}_{0.5}\text{N}$ even at 300 °C.

© 2007 WILEY-VCH Verlag GmbH & Co. KGaA, Weinheim

1 Introduction

In recent years, there has been increasing interest in AlGa_N-based light-emitting diodes (LEDs) and photodetectors operating in the deep-ultraviolet (UV) regime [1–5]. Plasma etching is an essential step in the fabrication of these deep-UV devices because a mesa structure must be defined for structures grown on insulating substrates such as sapphire. Low-damage etching processes are desirable as plasma damage may increase surface leakage and recombination [6]. Very little effort has been directed toward an understanding of the nature of plasma damage in AlGa_N, particularly AlGa_N with high Al mole fractions.

It is also important to understand the effects of plasma etching on the characteristics of ohmic contacts to AlGa_N since the n-type electrode of UV LEDs is typically formed on the plasma-etched surface. Previous studies showed that plasma treatment increased the surface doping level in n-type Ga_N and low-Al content AlGa_N due to preferential sputtering of N atoms [7–11]. Low-resistance ohmic contacts can be formed on n-Ga_N exposed to plasma even without annealing [9, 10]. As the Al mole fraction and thus the energy bandgap increases, it is increasingly difficult to produce low-resistance ohmic contacts to AlGa_N [12]. It is of high interest to find out if plasma damage has the same beneficial effects on metal contacts to AlGa_N with high Al mole fractions.

In this paper, the surface chemical and electronic properties of plasma-treated n- $\text{Al}_{0.5}\text{Ga}_{0.5}\text{N}$ are studied by X-ray photoemission spectroscopy (XPS) and electrical contact measurements, respectively. It is found that plasma treatment of $\text{Al}_{0.5}\text{Ga}_{0.5}\text{N}$ results in a N-deficient but compensated surface, degrading the quality of ohmic contacts.

* Corresponding author: e-mail: xacao@mail.wvu.edu

2 Experimental details

A 1 μm thick Si-doped ($n_{\text{Si}} = 5 \times 10^{18} \text{ cm}^{-3}$) $\text{Al}_{0.5}\text{Ga}_{0.5}\text{N}$ epilayer was grown on 2'' *c*-plane sapphire with a 0.5 μm AlN template using metalorganic chemical vapor deposition. The Al mole fraction was determined by the Ga and Al source flow rates, and the value measured by X-ray diffraction (XRD) was within 4% of nominal. The optical absorption edge was measured to be 4.88 eV. The room-temperature electron concentration and mobility, as determined by Hall measurements, were $2.7 \times 10^{18} \text{ cm}^{-3}$ and $50 \text{ cm}^2/\text{vs}$, respectively.

Three different samples were prepared by dicing the 2'' wafer into three equal pieces. All the samples were chemically cleaned using HCl:H₂O (1:1) and buffered oxide etch (BOE) solutions. The first, without further treatment, was used as the control. The second sample was etched in a Cl₂/BCl₃ inductively coupled plasma (ICP) for 1 min using a typical AlGa_xN etching recipe (5 mTorr base pressure, 300 W source power and 40 W rf chuck power). The etch rate was found to be 145 nm/min, as compared to 225 nm/min for GaN under the same condition. The third sample was exposed to an Ar ICP for 1 min (8 mTorr base pressure, 500 W source power and 150 W rf chuck power). The samples were characterized using XPS in an Axis Ultra delay-line detector system equipped with a monochromated Al K _{α} X-ray source. The Ga-3d, Al-2p, N-1s and O-1s peaks were recorded and the surface carbon, as represented by the C-1s peak, was used for calibration. To investigate surface electronic properties, a metal stack of Ti/Al/Ti/Au (30/120/30/200 nm) was deposited on the control and plasma-exposed samples using e-beam evaporation, and circular transmission-line-method (TLM) patterns with 5–45 μm gaps were formed by liftoff. The samples were then further cleaved into sections for 1 min rapid thermal annealing in N₂ at temperatures in the range of 600–1000 °C. Current–voltage (*I*–*V*) characteristics of the contacts were measured before and after the annealing using the four-point probe technique. In some cases, the *I*–*V* measurements were carried out at elevated temperatures up to 300 °C.

3 Results and discussion

3.1 Surface chemical analyses

Angle-dependent XPS measurements were carried out to determine the chemical composition profiles at the near-surface. At large angles, photoelectrons from the bulk are dominant, whereas at small angles the signal mainly originates from the surface. Figure 1 shows the integrated intensities of the Ga-3d, Al-2p, and O-1s

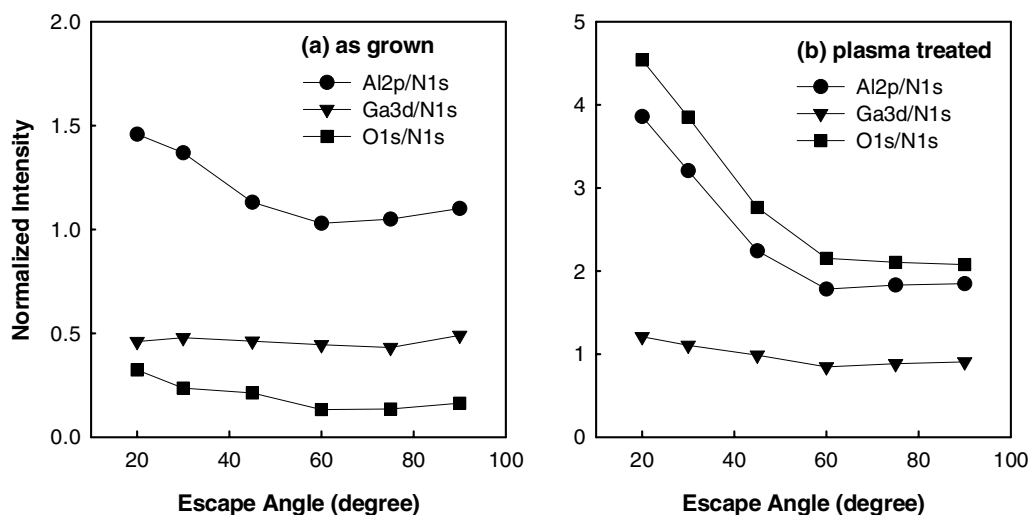


Fig. 1 Integrated intensities of Ga-3d, Al-2p, and O-1s photoelectron peaks normalized to the integrated N-1s intensity, as a function of electron escape angle, for (a) as-grown and (b) Ar plasma treated $\text{Al}_{0.5}\text{Ga}_{0.5}\text{N}$ samples.

and O-1s spectra normalized to the N-1s intensity as a function of electron escape angle. As seen in Fig. 1(a), the O concentration in the control sample is low, indicating that the native oxide was largely removed by the wet chemical clean. While the composition distribution of Ga is nearly constant, the Al-2p, and O-1s intensities exhibit a considerable increase at small angles. The latter suggests a nonstoichiometric AlGa_{0.5}N surface with Al–O rich and Ga–N deficient composition. After Ar plasma treatment, the O-1s intensity increases sharply, as shown in Fig. 1(b). The steep increases in the Al-2p, O-1s and Ga-3d at small angles indicate N is depleted in the topmost layer. The N-deficiency resulted from preferential sputtering of N during the plasma treatment, creating N vacancies. It has been found that ion-induced N vacancies in GaN act as shallow donors, leading to highly conductive n-GaN surfaces [7–11], or compensated p-GaN surfaces [13]. In this work, we find that N vacancies act as deep-level states in high-Al content AlGa_{0.5}N, as detailed below.

Figure 2 shows the spectra of the O-1s photoelectrons. The integrated intensity of the plasma-treated sample is $\sim 6.9 \times$ higher than that of the control sample. The amount of oxygen incorporation is higher than that has been observed in GaN materials upon plasma treatment [10, 14]. This is due in part to the higher propensity of AlN than GaN toward oxidation [15]. The O incorporation may occur during the plasma process due to the presence of residual O in the chamber. It may also take place during the subsequent exposure to ambient atmosphere [14]. The plasma-treated surface has a higher tendency to oxidize due to the preferential loss of N, leading to a nonstoichiometric surface with unsatisfied Al and Ga bonds. As seen in Fig. 2, the O-1s peak for the plasma-treated sample is asymmetrical with a shoulder at the higher binding energy, indicating unequal amounts of the Al–O and Ga–O components. The overall peak exhibits a significant red shift with respect to the peak for the control sample. To remove the surface oxide, the plasma-treated sample was etched in a HCl:H₂O (1:2) solution. The O-1s peak for the HCl-etched sample is also shown in Fig. 2. The peak intensity is markedly reduced, but the red shift is retained.

Figure 3 shows the XPS spectra of the Ga-3d core level for the control and plasma-treated samples, as well as the sample treated by plasma and HCl. The spectrum for the control sample corresponds to a dominant Ga–N component. Again, the Ga-3d spectrum of the plasma-treated sample is broad and asymmetrical, presumably due to an increased Ga–O component, which has a higher bonding energy than Ga–N. The Ga-3d peaks display a large shift toward the lower binding energy after the plasma and chemical treatments, from 20.13 eV to 19.45 eV, implying a 0.68 eV downward move of the Fermi level

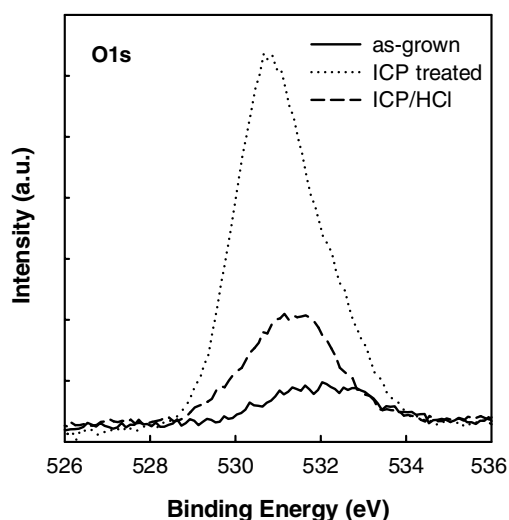


Fig. 2 XPS spectra of the O-1s core level for as-grown, Ar plasma-treated, and Ar plasma/HCl treated Al_{0.5}Ga_{0.5}N samples.

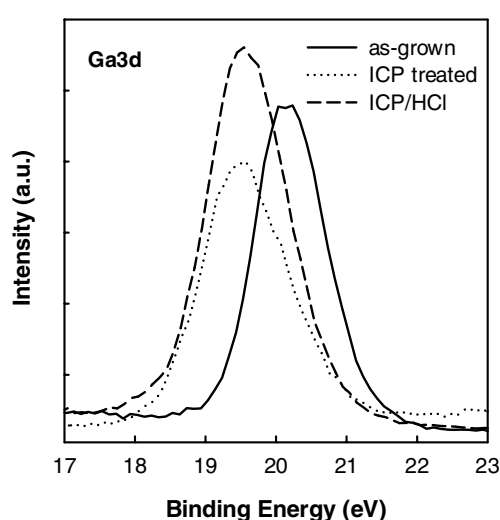


Fig. 3 XPS spectra of the Ga-3d core level for as-grown, Ar plasma-treated, and Ar plasma/HCl treated Al_{0.5}Ga_{0.5}N samples.

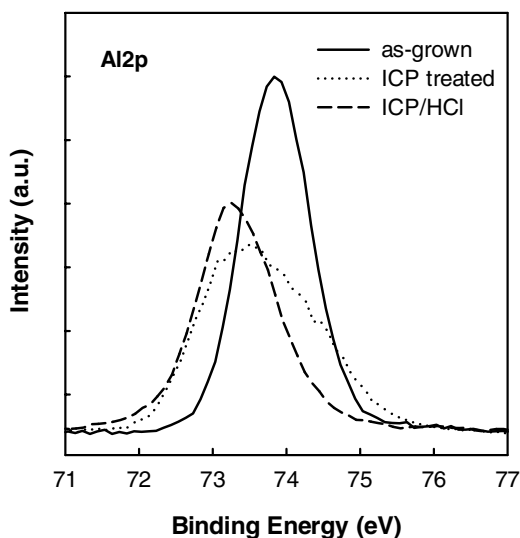


Fig. 4 XPS spectra of the Al-2p core level for as-grown, Ar plasma-treated, and Ar plasma/HCl treated $\text{Al}_{0.5}\text{Ga}_{0.5}\text{N}$ samples.

away from the conduction band at the surface. This is in sharp contrast to what has been observed in plasma-treated n-type GaN and low-Al AlGaN, where the Ga3d peak has been found to shift toward the higher binding energy, indicating that the surface Fermi level moves closer to the conduction band edge [10, 11, 14]. Interestingly, the removal of surface oxide by HCl has minimal impact on the peak shift. This suggests that the Fermi level movement arises from the change in bulk properties near the surface rather than surface oxidation. It is plausible that the energy level of plasma-induced defects in AlGaN, including N vacancies, deepens with increasing Al mole fraction, and plasma treatment introduces compensating defects rather than shallow donors in $\text{Al}_{0.5}\text{Ga}_{0.5}\text{N}$. The defects tend to pin the Fermi level, leading to a downward shift of the surface Fermi level.

The asymmetrical feature is even more noticeable in the Al-2p spectrum for the plasma-treated $\text{Al}_{0.5}\text{Ga}_{0.5}\text{N}$ as illustrated in Fig. 4. The control spectrum exhibits a single component Al-2p peak corresponding to Al–N bonds. The full width at half maximum of the peak is ~ 1.1 eV. The peak for the plasma-treated surface is much broader, and can be decomposed into two major Gaussian peaks, with the higher binding energy peak corresponding to Al–O. The chemical shift between the two peaks is ~ 1.0 eV, in good agreement with previous reports [16, 17]. As also seen in Fig. 4, the post-treatment HCl cleaning nearly eliminates the Al–O component. The spectrum exhibits a single-component peak corresponding to Al–N, with a redshift of ~ 0.6 eV with respect to the control Al-2p peak.

3.2 Electrical characterization

To gain insight into the effects of plasma treatment on surface electronic properties of AlGaN, the characteristics of ohmic contacts formed on the control and treated samples were examined. Figure 5(a) shows the I – V characteristics of the contacts on the control $\text{Al}_{0.5}\text{Ga}_{0.5}\text{N}$ sample after annealing at various temperatures ranging from 600–1000 °C. The as-deposited contact exhibits leaky Schottky characteristics, and the annealed contacts remain Schottky. Annealing at 600 °C and 700 °C actually degrades the I – V characteristics slightly. The current peaks at 800 °C, but is only slightly higher than that in the as-deposited contact. The solid-phase reactions, which take place during the annealing are believed to be similar to the case of Ti-based contacts to n-GaN [6, 18]. They may include (i) the dissolution of remaining native oxides by Ti; (ii) the outdiffusion of N and the subsequent formation of a N-deficient interfacial layer; (iii) the formation of low-work function Ti–N and other interfacial alloys. The degraded I – V characteristics for the contacts annealed above 800 °C suggest that the interfacial reactions, including N outdiffusion, may have an adverse effect on the contact property.

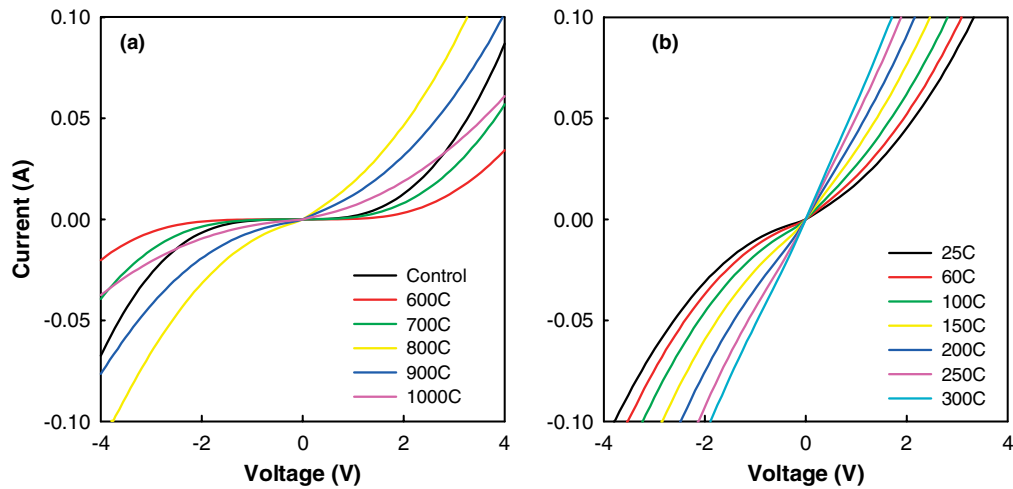


Fig. 5 (online colour at: www.pss-a.com) (a) I – V characteristics of Ti/Al/Ti/Au contacts to as-grown $\text{Al}_{0.5}\text{Ga}_{0.5}\text{N}$ after annealing at various temperatures in N_2 , (b) I – V characteristics of the 900 °C-annealed Ti/Al/Ti/Au contact measured at 25–300 °C.

Figure 5(b) shows the I – V characteristics of the contact annealed at 900 °C and measured at temperatures from 25–300 °C. The contact becomes ohmic at 250 °C, with a specific contact resistance of $2.6 \times 10^{-3} \Omega \text{ cm}^2$. As the temperature increases, both thermionic emission over the Schottky barrier and electron tunneling across the barrier increase. While the ionization energy of Si in AlGaN increases with increasing Al content, it remains very low in $\text{Al}_{0.5}\text{Ga}_{0.5}\text{N}$, $\sim 12 \text{ meV}$ [19]. Si acts as a shallow donor in $\text{Al}_{0.5}\text{Ga}_{0.5}\text{N}$ and is almost fully ionized even at room temperature. The ohmic behavior of the contact is therefore due largely to more efficient thermionic emission at elevated temperatures.

Figure 6(a) and (b) compares the I – V characteristics of the contacts on Cl_2/BCl_3 and Ar plasma-treated samples before and after annealing at 900 °C. The I – V curves of the contacts on the control samples are also shown for comparison. The plasma treatment significantly degrades the contact characteristics. The contacts on the plasma-treated samples become more rectifying, indicating a decreased surface conductivity as a result of the plasma exposure. This is in contrast to the previous findings that plasma

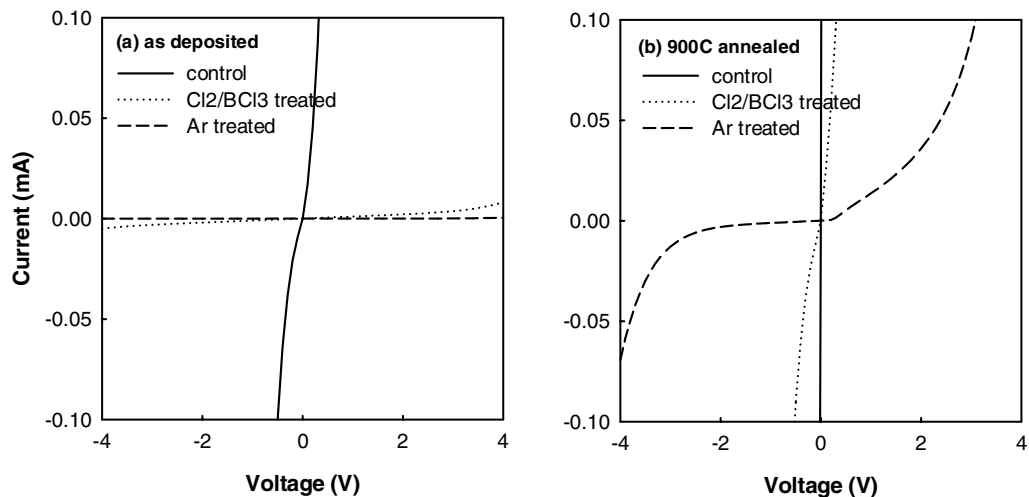


Fig. 6 I – V characteristics of Ti/Al/Ti/Au contacts to plasma-treated $\text{Al}_{0.5}\text{Ga}_{0.5}\text{N}$ (a) before and (b) after annealing at 900 °C in N_2 .

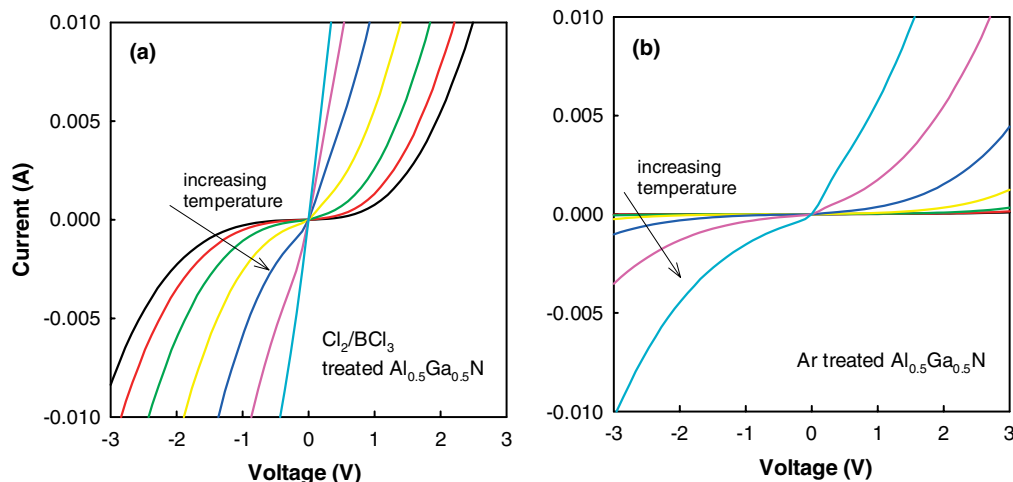


Fig. 7 (online colour at: www.pss-a.com) I - V characteristics of Ti/Al/Ti/Au contacts to plasma-treated $\text{Al}_{0.5}\text{Ga}_{0.5}\text{N}$, annealed at $900\text{ }^{\circ}\text{C}$ in N_2 and measured at 25 - $300\text{ }^{\circ}\text{C}$.

treatment improves the contact quality on GaN due to ion-induced N vacancies acting as shallow donors in GaN [10, 11]. Note that Ar plasma has a greater impact on the electrical properties of the contacts than Cl_2/BCl_3 plasma. This is because that, during the Ar plasma treatment, a higher flux of more energetic ions is involved and plasma damage is accumulating with little concurrent etching of the material.

Since the surface oxide can largely be dissolved by Ti during the anneal, we do not think it accounts for the degraded performance of the contacts on plasma treated surfaces. The deteriorated contact characteristics can be explained by the above XPS analysis results. The characterization of the surface bonding states shows a downward shift of the surface Fermi level in plasma-treated $\text{Al}_{0.5}\text{Ga}_{0.5}\text{N}$, suggesting that plasma-induced defects act as deep-level states, pinning the Fermi level. As a result, the Schottky barrier is increased and current conduction via tunneling is suppressed, leading to more rectifying contact characteristics. As seen in Fig. 6, the damage can not be completely removed by annealing at $900\text{ }^{\circ}\text{C}$.

Figure 7 shows the I - V characteristics of the contacts formed on the Cl_2/BCl_3 and Ar plasma treated samples, annealed at $900\text{ }^{\circ}\text{C}$ and measured at elevated temperatures. The contact to Cl_2/BCl_3 treated sample improves with increasing ambient temperature, and becomes ohmic at $300\text{ }^{\circ}\text{C}$. However, the I - V characteristics of the contact to the Ar plasma-treated sample remain nonlinear at $300\text{ }^{\circ}\text{C}$, suggesting strong compensation effects even at this temperature. These findings emphasize the need to mitigate plasma damage introduced during the mesa etch step for AlGaN-based deep-UV emitters and detectors.

4 Conclusions

In summary, the surface chemical and electronic properties of plasma-treated $\text{Al}_{0.5}\text{Ga}_{0.5}\text{N}$ were studied. XPS analyses revealed a N-deficient nonstoichiometric surface, which can be readily oxidized. Ion-induced damage can not be annealed out at $900\text{ }^{\circ}\text{C}$ and acts as deep-level compensation centers in $\text{Al}_{0.5}\text{Ga}_{0.5}\text{N}$, leading to a downward shift of the surface Fermi level and a reduced surface conductivity. Pre-metal plasma treatment results in more rectifying electrical characteristics of Ti/Al/Ti/Au contacts to n- $\text{Al}_{0.5}\text{Ga}_{0.5}\text{N}$. Increasing in-situ Si doping and minimizing plasma damage are therefore essential for producing good-quality ohmic contacts to AlGaN with high Al mole fractions.

References

- [1] A. A. Allerman, M. H. Crawford, A. J. Fischer, K. H. A. Bogart, S. R. Lee, D. M. Follstaedt, P. P. Provencio, and D. D. Koleske, *J. Cryst. Growth* **272**, 227 (2005).
- [2] J. P. Zhang, X. Hu, Y. Bilenko, J. Deng, A. Lunev, M. Shur, R. Gaska, M. Shatalov, J. W. Yang, and M. Asif Khan, *Appl. Phys. Lett.* **85**, 5532 (2004).

- [3] X. A. Cao, S. F. LeBoeuf, and T. E. Stecher, *IEEE Electron Device Lett.* **27**, 329 (2006).
- [4] A. Chitnis, J. Sun, V. Mandavilli, R. Pachipulusu, S. Wu, M. Gaevski, V. Adivarahan, J. P. Zhang, M. A. Khan, A. Sarua, and M. Kuball, *Appl. Phys. Lett.* **81**, 3491 (2002).
- [5] R. McClintock, A. Yasan, K. Mayes, D. Shiell, S. R. Darvish, P. Kung, and M. Razeghi, *Appl. Phys. Lett.* **84**, 1248 (2004).
- [6] H. S. Yang, S. Y. Han, K. H. Baik, S. J. Pearton, and F. Ren, *Appl. Phys. Lett.* **86**, 102104 (2005).
- [7] X. A. Cao, S. J. Pearton, G. T. Dang, A. P. Zhang, F. Ren, and J. M. Van Hove, *IEEE Trans. Electron Devices* **47**, 1320 (2000).
- [8] X. A. Cao, F. Ren, and S. J. Pearton, *Crit. Rev. Solid State Mater. Sci.* **25**, 279 (2000).
- [9] Z. Fan, S. N. Mohammad, W. Kim, Ö. Aktas, A. E. Botchkarev, and H. Morkoç, *Appl. Phys. Lett.* **68**, 1672 (1996).
- [10] H. W. Jang, C. M. Jeon, J. K. Kim, and J. L. Lee, *Appl. Phys. Lett.* **78**, 2015 (2001).
- [11] X. A. Cao, H. Piao, and S. F. LeBoeuf, J. Li, J. Y. Lin, and H. X. Jiang, *Appl. Phys. Lett.* **89**, 082109 (2006).
- [12] S. Ruvimov, Z. Liliental-Weber, J. Washburn, D. Qiao, S. S. Lau, and P. K. Chu, *Appl. Phys. Lett.* **73**, 2582 (1998).
- [13] X. A. Cao, S. J. Pearton, A. P. Zhang, G. T. Dang, F. Ren, R. J. Shul, L. Zhang, R. Hickman, and J. M. Van Hove, *Appl. Phys. Lett.* **75**, 2569 (1999).
- [14] D. Selvanathan, F. M. Mohammed, J. O. Bae, I. Adesida, and K. H. Bogart, *J. Vac. Sci. Technol. B* **23**, 2538 (2005).
- [15] S. A. Nikishin, B. A. Borisov, A. Chandolu, V. V. Kuryatkov, H. Temkin, M. Holtz, E. N. Mokhov, Y. Makarov, and H. Helava, *Appl. Phys. Lett.* **85**, 4355 (2004).
- [16] T. Hashizume, S. Ootomo, S. Oyama, M. Konishi, and H. Hasegawa, *J. Vac. Sci. Technol. B* **19**, 1675 (2001).
- [17] C. I. Wu, A. Kahn, E. S. Hellman, and D. N. E. Buchanan, *Appl. Phys. Lett.* **73**, 1346 (1998).
- [18] A. Motayed, R. Bathe, M. C. Wood, O. S. Diouf, R. D. Vispute, and S. Noor Mohammad, *J. Appl. Phys.* **93**, 1087 (2003).
- [19] Y. Taniyasu, M. Kasu, and N. Kobayashi, *Appl. Phys. Lett.* **81**, 1255 (2002).